Engineering the Electronic Structure in Titanium Dioxide via Scandium Doping Based on the Density Functional Theory Approach for the Photocatalysis and Photovoltaic Applications

Singh, Ram Sevak*[+]

Department of Physics, OP Jindal University, Raigarh, Chhattisgarh-496109, INDIA

Gautam, Anurag

Department of Chemistry, Geethanjali College of Engineering and Technology, Cheeryal, Hyderabad, Telangana-501301, INDIA

Rai, Varun

Department of Chemistry, 3 Science Drive 3, National University of Singapore, 117543, SINGAPORE

ABSTRACT: *Titanium dioxide (TiO_2) has received much attention, owing to applications in various areas including photocatalysis and photovoltaics. It is a wide band gap n-type semiconductor. Production of p-type TiO_2 is challenging and interesting research work for its utilization in wider areas of applications. In this study, band structures and corresponding density of states of undoped and scandium (Sc)-doped TiO_2 with different concentrations of Sc doping are calculated using Density Functional Theory (DFT). Sc doping in TiO_2 converts intrinsically n-type TiO_2 into p-type TiO_2. An increase in doping concentration generates shallow acceptor levels ranging from 10 meV to 25 meV above the Fermi level. The study has the potential to improve the conductivity of TiO_2 via different concentrations of Sc dopants and produce p-type TiO_2 for applications in photocatalytic water-splitting technology in low-cost and eco-friendly hydrogen production and solar cell technology to support future energy demand.*

KEYWORDS: *Density functional theory; p-type doping; Electronic properties; Hydrogen energy; Fuel cell.*

INTRODUCTION

The catalytic process is vital in the field of materials chemistry because the outcome of a chemical reaction is controlled by the application of a suitable catalyst. Usually, at the nanoscale, the catalyst can provide a more powerful strategy in a given environment to achieve the goal due to quantum confinement [1]. Different nanoscale materials have been utilized for potential applications in various sectors [2-6]. In particular, metal oxide

** To whom correspondence should be addressed.*
+ E-mail: singh915@gmail.com
1021-9986/2023/3/731-739 9/$/5.09

nanoparticles such as TiO_2, ZnO, WO_3 have been extensively used for photocatalytic, catalytic, and photovoltaic applications due to the easier synthesis process, nontoxicity, high chemical stability, and abundance nature [7]. TiO_2 has mainly three polymorphs as anatase, rutile, and brookite, out of those anatase and rutile are the most common in nature [8]. At the nanoscale, the stability of the anatase is higher than another polymorph therefore, it is the most interesting phase that has received much more attention from scientists and engineers due to its intriguing widespread applications in many fields that include photocatalysis and photovoltaic devices [9-13].

The anatase TiO_2 is a wide band gap semiconductor material with a band gap of 3.23 eV [14]. Therefore, for its more efficient application, tuning of electronic and magnetic properties is certainly needed. Usually, the electronic properties are getting tuned by the controlled introduction of the dopants and the defects in the TiO_2 matrix that are associated with the trapping or the self-trapping phenomenon. Subsequently, the doped TiO_2 produced would have more peculiar properties than the parent TiO_2 system. For this reason, doped TiO_2 is one of the most widely studied materials both theoretically and experimentally. The combined outcome of the theoretical and computation work would lead to a clear idea of the complex doped system for their future advancement and better understanding [15].

A literature review suggested that the doped TiO_2 has good photocatalytic activity. For instance, *Livraghi et al.* [16] have reported nitrogen-doped TiO_2 nanoparticles that have paramagnetic centers (neutral NO radicals and NO_2-type radicals) were capable of decomposing the organic pollutant using visible light. In another attempt, *Wei et al.* [15] synthesized TiO_2 nanoparticles co-doped with nitrogen and lanthanum (La3+) ions. The doping of nitrogen resulted in narrowing the band gap of TiO_2 which enhanced the absorption between 350 nm to 450 nm due to the superior catalytic activity while the doping of La^{3+} ions increases the surface area of the sample further increasing the absorption below 350 nm. The electrical conductivity of TiO_2 thin film is improved via Sc-doping [17].

The use of machine learning in material science, physics, and chemistry is increasing [18-25]. It uses techniques and algorithms to solve various complex problems which are difficult to solve using traditional programming methods. Various high-performance organic solar cells have been demonstrated using machine learning. In the context of TiO_2, several experimental as well as theoretical studies have been reported to alter the electronic property of TiO_2 [26-33]. *Cavalheiro et al.* [28] experimentally observed that the photocatalytic property of TiO_2 is improved due to Sc-doping. However, most of the previous reports lack details of Sc-doping into TiO_2 to get more insight into the observed phenomena. Details about the effect of an increase in dopant concentration on the electronic structure, whether the doping is n-type or p-type, calculation of impurity ionization energy, and localization of a charge carrier and their applications in solar cells are yet to be explored. Hence, a detailed theoretical study on the influence of varying Sc doping concentration into TiO_2 on its electronic property is needed.

In this article, a systematic study on the influence of Sc-doping on the electronic properties of anatase TiO_2 is carried out using first-principle calculations based on density functional theory (DFT). The calculated results show the p-type doping of TiO_2, and the density of states (DOS) in the valence band and the vicinity of Fermi level increases with an increase in dopant concentration. Furthermore, with an increase in Sc concentration, acceptor levels are generated above the Fermi level at the most symmetric G-point. Positions of acceptor energy levels, doping concentrations, and carrier localization are calculated and discussion on their importance for photocatalytic and solar cell applications is also well explored. The research findings, presented in this paper, underscore the impact of Sc doping concentration on the alteration of electronic structures of anatase TiO_2. The study may be utilized further in various experimental work and applications such as using it as photocatalysts of hydrogen production and as active materials in solar cells.

EXPERIMENTAL SECTION

The anatase phase of TiO_2 has a tetragonal structure with space group 141/AMD. Lattice constants are a = b = 0.3785 nm, c = 0.9514 nm; $\alpha = \beta = \gamma = 90^o$ [14]. The electronic structures of undoped and Sc-doped TiO_2 were studied using the first principles of calculation based on density functional theory. DFT calculations were performed using the Cambridge Sequential Total Energy Package (CASTEP) in Materials Studio 7. The method comprised of geometry optimization of anatase TiO_2 structures with and without

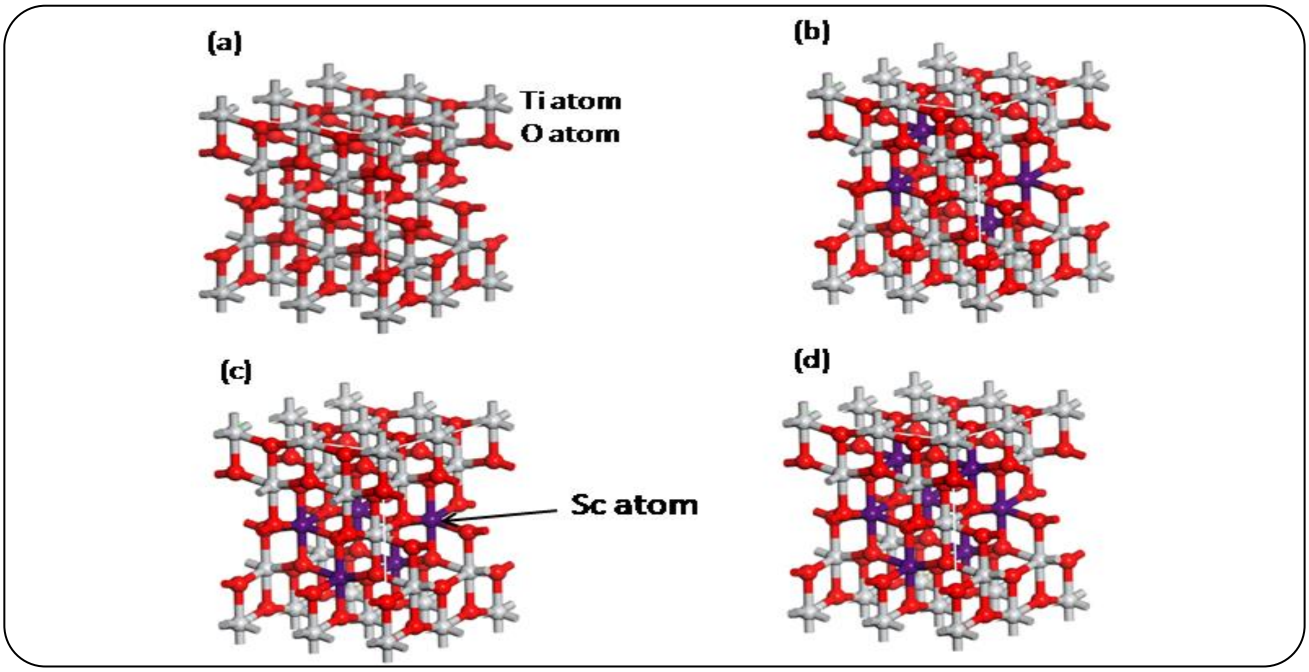

***Fig. 1.** 2×2×1 supercell models of undoped anatase TiO_2 and Sc doped TiO_2.(a) Undoped TiO_2, (b) TiO_2 doped with 8.33 at.% of Sc ($Ti_{12}Sc_4O_{32}$), (c) TiO_2 doped with 10.43 at.% of Sc ($Ti_{11}Sc_5O_{32}$), and (d) TiO_2 doped with 14.58 at.% of Sc ($Ti_9Sc_7O_{32}$). Sc atoms are indicated with a violet color.*

Sc doping. All geometry optimizations were performed in a uniform 3×3×1 k-point mesh in the Brillouin zone using plane-wave ultrasoft pseudopotential with a cut-off energy of 240 eV until the force on each atom is less than 0.05 eV/Å.

The exchange-correlation is described by generalized gradient approximation (GGA) [34]. The lattice constants of the optimized TiO_2 unit cell are found to be a = b = 0.381 nm, c = 0.958 nm which are matching with the lattice constants reported in the literature [14].

RESULTS AND DISCUSSION

In the presented results, to realize the doping of Sc in different concentrations, a 2×2×1 supercell model was designed as shown in Fig. 1. The tetragonal structure of TiO_2 consists of 4 Ti atoms and 8 O atoms in a unit cell. The supercell 2×2×1 designed in this study has stacks off our unit cells which consist of 16 Ti and 32 O atoms with a total of 48 atoms as shown in Fig. 1a. For different dopant concentrations, the different nnumbers of c atoms were substituted at Ti sites. The number of Sc atoms (say N_{Sc}) for substitution was chosen as N_{Sc}= 4 (Fig. 1b), N_{Sc} = 5 (Fig. 1c), and N_{Sc} = 7 (Fig. 1d). The concentration of Sc dopants in atomic percentage was calculated as $(N_{Sc}/N_T)\times100$, where N_T (= 48) is the total number of atoms in the 2×2×1 supercell. Thus, substitutions of 4, 5, and 7 atoms of Sc correspond to concentrations of 8.33%, 10.43%, and 14.58% respectively. Stabilities of the undoped and Sc-doped TiO_2 were studied by performing total energy (ground state energy) calculations in fully relaxed geometries (Fig. 1) with fixed parameters. The total energy is found to be −40622.84 eV for undoped TiO_2, −41332.18 eV for 8.33% Sc-doped TiO_2, -41743.55 eV for 10.43% Sc-doped TiO_2 and −41880.27 eV for 14.58% Sc-doped TiO_2. It is noticed that ground state energies of Sc-doped TiO_2 are higher than that of undoped TiO_2, indicating that the stability of the TiO_2 increases due to Sc-doping.

To study the electronic properties, calculations for band structures of undoped TiO_2 and TiO_2 doped with different concentrations of 8.33 % (Sc/TiO_2 8.33%), 10.43% (Sc/TiO_2 10.43%), and 14.58 % (Sc/TiO_2 14.58 %) were performed by optimizing the structures using appropriate parameters detailed in the Experimental Section. The calculated results of band structures are presented in Fig. 2. The G, F, Q, and Z in band structures of Fig. 2 are different k-points in the Brillouin zone. From Fig. 2a, the band gap of undoped TiO_2 which is the energy

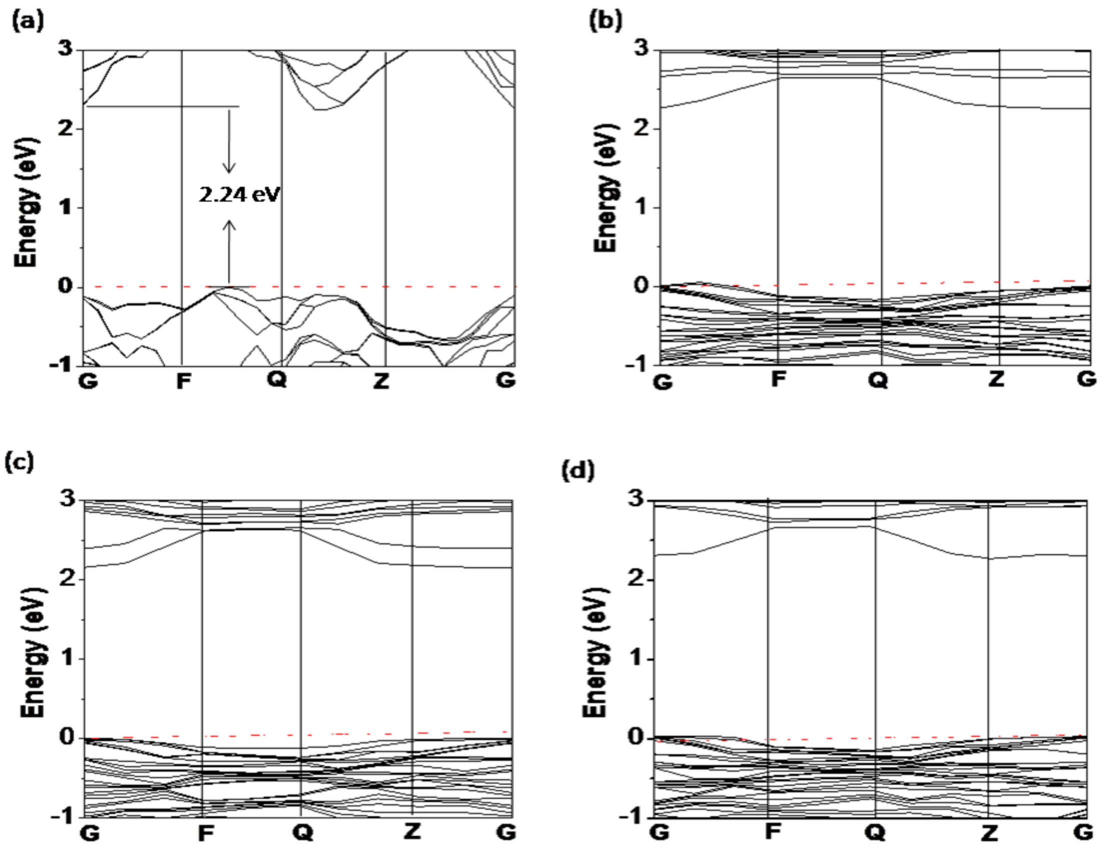

***Fig. 2:** Band structures of (a) undoped TiO_2, (b) Sc/TiO_2 8.33 at.%, (c) Sc/TiO_2 10.43 at.%, (d) Sc/TiO_2 14.58 at.%. The Fermi level is set to zero and indicated by the dotted red line.*

between Valence Band Maximum (VBM) and Conduction Band Minimum (CBM) was calculated to be 2.24 eV. The VBM is located between F and Q while CBM is located at G. This indicates that TiO_2 has an indirect band gap. The band gap of undoped TiO_2 calculated in this study is well agreed with theoretical results by another group [35]. However, the calculated band gap is much smaller than the experimental band gap of 3.23 eV. The underestimation of this band gap is attributed to the intrinsic feature of the Generalized Gradient Approximation (GGA) adopted in our calculation. Fig. 2b-d shows the band structures of Sc-doped TiO_2 with the three different concentrations (8.33%, 10.43%, and 14.58%) of Sc. In Figs. 2b-d, we see that the Valence Band (VB) is relatively flat as compared to the conduction band. A flat band of VB indicates the localization of particles (holes) due to the incorporation of Sc impurity. Quantum destructive interference of carrier wave function on the lattice can cause this carrier localization (effective mass of carrier tends to be infinite), resulting in flattening of bands in VB. Another noticeable feature is the increase in the number of energy levels in VB which makes the band denser (see Figs. 2b-d). The increased number of energy levels in VB due to the Sc-doping is an indication of p-type doping of TiO_2. Doping Sc at the Ti site can result in p-type doping that can be understood as follows. The atomic number of Sc is 21 while the atomic number of Ti is 22. Thus, Sc has 3 valence electrons $4s^2$, $3d^1$ while Ti has 4 valence electrons $4s^2$, $3d^2$ considering the participation of 3d electrons. If we replace the Sc atom at the Ti site, 3 electrons of Ti will be involved in making a covalent bond by sharing 3 electrons from Sc. However, the 4^{th} electron of Ti lacks one electron (absence of an electron that is called a hole) from Sc to share and hence to form a covalent bond. Thus, substituting one Sc atom into the TiO_2 crystal at the Ti site leaves one hole or absence of an electron in the crystal.

To get more insight into the electronic structure, the data in Fig. 2 is enlarged near the Fermi level (shown by a dotted red line) at G which is presented in Fig. 3. For TiO_2 doped with 8.33 % of Sc (see Fig. 3b), it is found that an electronic state of VB crosses the Fermi level near the

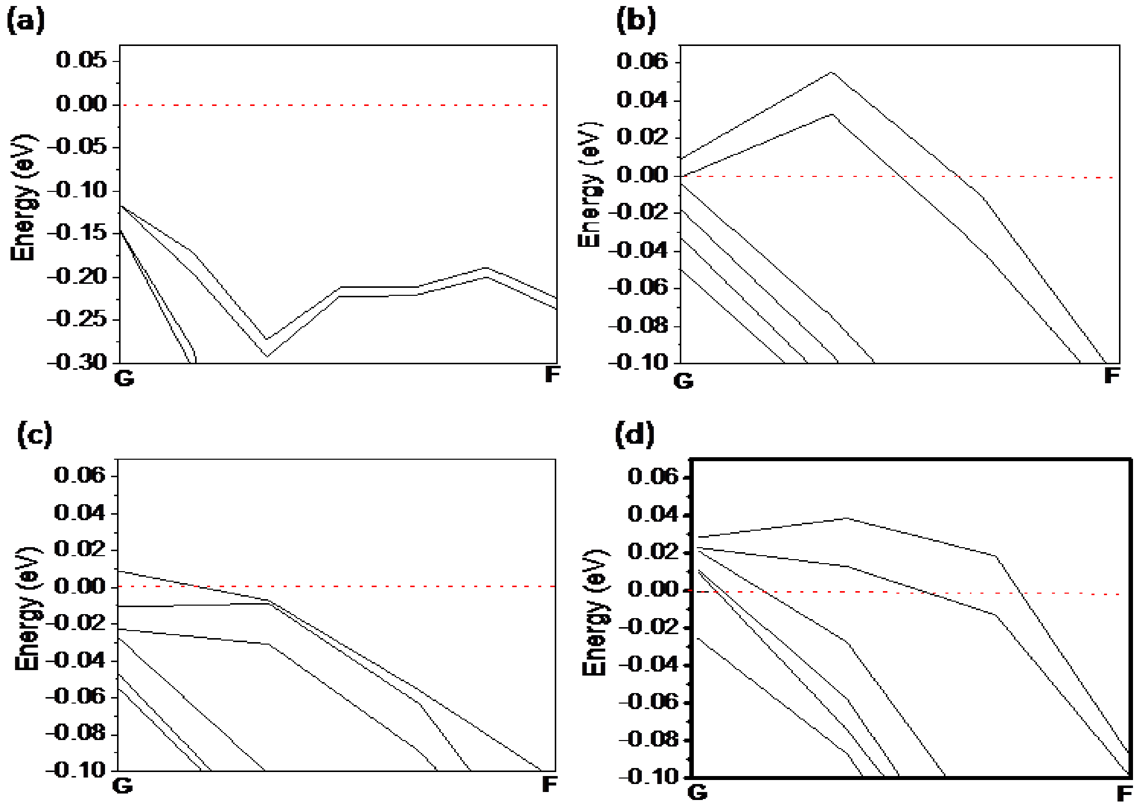

***Fig. 3:** Enlarged view of band structures shown in Fig. 2 near Fermi level for (a) undoped TiO_2, (b) Sc/TiO_2 8.33 at.%, (c) Sc/TiO_2 10.43 at.%, (d) Sc/TiO_2 14.58 at.%. The Fermi level is set to zero and indicated by the dotted red line.*

most symmetric G point and this state has an energy of 10 meV above the Fermi level at G point. Fig. 3d shows that for Sc concentration of 14.58% there are five states of VB near the G point which cross the Fermi Level. These energy levels are shallow acceptor energy levels lying in the range from 10 meV to 25 meV above the Fermi level.

Thus, calculated acceptor ionization energy lies in the range of 10-25 meV which is of the order of thermal energy at room temperature. It is noticed that carrier (hole) concentration increases in TiO_2 due to Sc doping. An increase in carrier concentration is one of the most important routes for improving the catalytic activity of semiconductor photocatalysts and efficiency of photovoltaic devices.

The Density Of States (DOS) of undoped TiO_2 and TiO_2 doped with different concentrations of Sc were also calculated. The results of DOS are presented in Fig. 4. In comparison with undoped TiO_2 (see Fig. 4a), TiO_2 doped with 8.33 % of Sc (see Fig. 4b) exhibits an increase of density of states (DOS) in VB, indicating p-type doping.

This result of DOS supports the calculations of band structures in Fig. 2 and Fig. 3. Similarly, by increasing the Sc concentration to 10.43% and 14.58%, DOS continued to increase further in VB as shown in Fig. 4c and Fig. 4d, respectively. This increase in DOS is also seen in the vicinity of the Fermi level (see the enlarged view on the right panel), indicating the generation of new impurity states due to the Sc doping which again supports the results of band structures presented in Fig. 2 and Fig. 3. An increase of carriers (holes) due to Sc doping dramatically increases the electrical conductivity of TiO_2 and also photocatalytic property as evidenced experimentally [17, 28]. Furthermore, we also find that the shape of DOS (considering DOS as Gaussian shape) changes after Sc doping as seen in the enlarged view on the right panels in Fig. 4. DOS shape of Sc-doped TiO_2 becomes narrower than that of undoped TiO_2. This narrowing of DOS peaks of VB near Fermi level is more obvious for 14.58 at.% doping of Sc as shown in the right panel of Fig. 4(d). This indicates that the electronic nonlocality is less obvious, owing to the increase of crystal symmetry [36] and localization of holes,

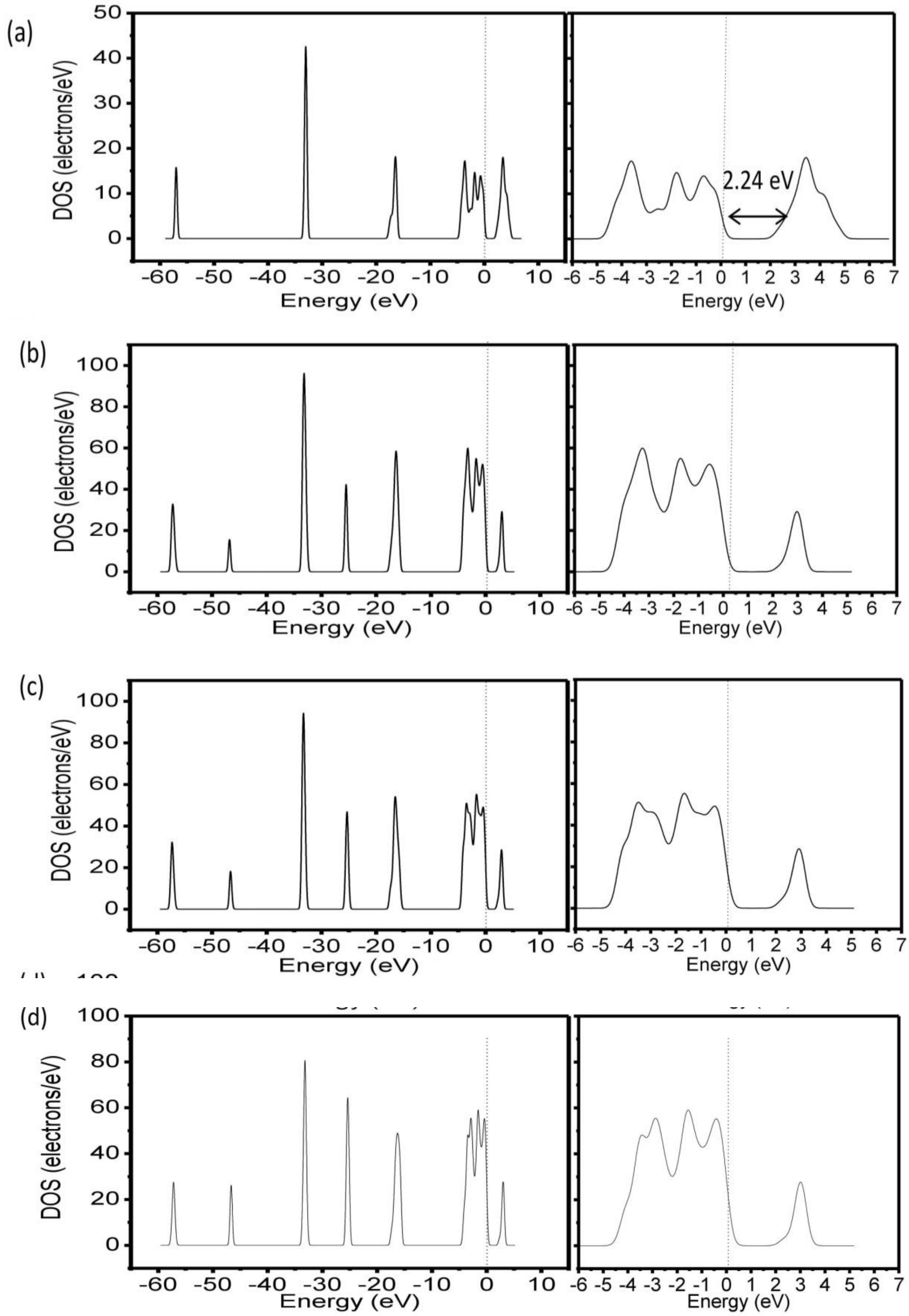

Fig. 4: Density of states (DOS) of (a) undoped TiO_2 (b) Sc/TiO_2 8.33 at.%, (c) Sc/TiO_2 10.43 at.%, (d) Sc/TiO_2 14.58 at.%. Fermi level is set to zero and presented by a dotted line. Where at.% stands for atomic%. The enlarged view of DOS near the Fermi level is shown on the right panel.

which is also supported by the flattening of energy levels in VB as shown by band structures (see Fig. 2(b-d)). Charge carrier localization has a significant impact on solar cell devices. Localization of holes as compared to the electron leads to the separation of electron-hole pairs, which dramatically improves the efficiency of a solar cell. Thus, our study here may further be employed to fabricate new and efficient solar cells in the future.

CONCLUSIONS

In summary, the electronic properties of Sc-doped anatase TiO_2 have been studied systematically using first-principle calculations based on density functional theory. Energy band structures and density of states of undoped TiO_2 and Sc-doped TiO_2 with varying concentrations of dopants are calculated. The results exhibit that Sc doping into TiO_2 causes p-type doping, which generates shallow acceptor levels lying in the range of 10 meV-25 meV above the Fermi level. It is also noticed that, with an increase in dopant concentration, the density of states in the valance band and the vicinity of the Fermi level increases, and the localization of holes occurs. The study is important because it highlights the influence of different concentrations of Sc doping into TiO_2, and it may further be applied to explore the dopant concentration-dependent alteration of electronic properties of TiO_2 for photocatalytic and photovoltaic applications.

Acknowledgments

The author acknowledges OP Jindal University, Raigarh, Chhattisgarh-496109, India to encourage and support for doing the research.

Received : Feb. 15, 2022 ; Accepted : May 30, 2022

REFERENCES

[1] Gao Z., Qin Y., Design and Properties of Confined Nanocatalysts by Atomic Layer Deposition, *Acc. Chem. Res*, **50(9)**: 2309-16 (2017).

[2] Edelstein A.S., Cammaratra R., "Nanomaterials: Synthesis, Properties and Applications", CRC Press (1998).

[3] Singh R.S., Li D., Xiong Q., Santoso I., Yu X., Chen W., et al., Anomalous Photoresponse in the Deep-Ultraviolet Due to Resonant Excitonic Effects in Oxygen Plasma Treated Few-Layer Graphene, *Carbon*, **106**: 330-335 (2016).

[4] Singh R.S., Gautam A., Rai V., Graphene-Based Bipolar Plates for Polymer Electrolyte Membrane Fuel Cells, *Front. Mater. Sci*., **13(3)**: 217-241 (2019).

[5] Singh R.S., Jansen M., Ganguly D., Kulkarni G.U., Ramaprabhu S., Choudhary S.K., et al., Shellac Derived Graphene Films on Solid, Flexible, and Porous Substrates for High Performance Bipolar Plates and Supercapacitor Electrodes, *Renew. Energy*, **181**: 1008-1022 (2022).

[6] Singh R.S., Rasheed A., Gautam A., Singh A.K., Rai V., Enhanced Optical and Electrical Properties of Graphene Oxide-Silver Nanoparticles Nanocomposite Film by Thermal Annealing in the Air, *Russ. J. Appl. Chem*., **94(3)**: 402-409 (2021).

[7] Di Valentin C., Pacchioni G., Spectroscopic Properties of Doped and Defective Semiconducting Oxides from Hybrid Density Functional Calculations, *Acc. Chem. Res*., **47(11)**: 3233 (2014).

[8] Li Y.-F., Aschauer U., Chen J., Selloni A., Adsorption and Reactions of O_2 on Anatase TiO_2, *Acc. Chem. Res*., **47(11)**: 3361-3368 (2014).

[9] Mora-Sero I., Giménez S., Fabregat-Santiago F., Gómez R., Shen Q., Toyoda T., et al. Recombination in Quantum Dot Sensitized Solar Cells, *Acc. Chem., Res*., **42(11)**: 1848-1857 (2009).

[10] Dong S., Feng J., Fan M., Pi Y., Hu L., Han X., et al., Recent Developments in Heterogeneous Photocatalytic Water Treatment Using Visible Light-Responsive Photocatalysts: A Review, *RSC Adv*., **5(19)**: 14610-14630 (2015).

[11] Gao M., Zhu L., Ong W.L., Wang J., Ho G.W., Structural Design of TiO_2-Based Photocatalyst for H_2 Production and Degradation Applications, *Catal. Sci. Technol*., **5(10)**: 4703-4726 (2015).

[12] Chen B., Meng Y., Sha J., Zhong C., Hu W., Zhao N., Preparation of MoS_2/TiO_2 Based Nanocomposites for Photocatalysis and Rechargeable Batteries: Progress, Challenges, and Perspective, *Nanoscale*, **10(1)**: 34-68 (2018).

[13] Ni M., Leung M.K., Leung D.Y., Sumathy K., A Review and Recent Developments in Photocatalytic Water-Splitting Using TiO_2 for Hydrogen Production, *Renew. Sustain. Energy Rev*., **11(3)**: 401-425 (2007).

[14] Asahi R., Taga Y., Mannstadt W., Freeman A., Electronic and Optical Properties of Anatase TiO_2, *Phys. Rev. B*, **61(11)**: 7459 (2000).

[15] Wei H., Wu Y., Lun N., Zhao F., Preparation and Photocatalysis of TiO_2 Nanoparticles Co-Doped with Nitrogen and Lanthanum, *J. Mater. Sci*., **39(4)**: 1305-1308 (2004).

[16] Livraghi S., Votta A., Paganini M.C., Giamello E., The Nature of Paramagnetic Species in Nitrogen Doped TiO_2 Active in Visible Light Photocatalysis, *Chem .Commun*., **(4)**: 498-500 (2005).

[17] Inoue T., Okumura T., Shimazu Y., Sakai E., Kumigashira H., Higuchi T., Electrical Conductivity of Sc-Doped TiO_2 Thin Film Prepared by RF Magnetron Sputtering, *Jpn. J. Appl. Phys*., **53(6S)**: 06JG3 (2014).

[18] Mahmood A., Wang J.-L., Machine Learning for High Performance Organic Solar Cells: Current Scenario and Future Prospects, *Energy Environ. Sci.*, **14(1)**: 90-105 (2021).

[19] Mahmood A., Wang J.-L., A Time and Resource Efficient Machine Learning Assisted Design of Non-Fullerene Small Molecule Acceptors for P3HT-Based Organic Solar Cells and Green Solvent Selection, *J. Mater. Chem. A*, **9(28)**: 15684-15695 (2021).

[20] Mahmood A., Irfan A., Wang J.L., Developing Efficient Small Molecule Acceptors with sp^2-Hybridized Nitrogen at Different Positions by Density Functional Theory Calculations, Molecular Dynamics Simulations and Machine Learning, *Chem. Eur. J.*, **28(2)**: e202103712 (2022).

[21] Mahmood A., Irfan A., Wang J.-L., Machine Learning and Molecular Dynamics Simulation-Assisted Evolutionary Design and Discovery Pipeline to Screen Efficient Small Molecule Acceptors for PTB7-Th-Based Organic Solar Cells with Over 15% Efficiency, *J. Mater. Chem. A*, **10(8)**: 4170-4180 (2022).

[22] Singh R.S., Sulfur-Doped Silicon Carbide Nanotube as a Sensor for Detecting Liquefied Petroleum Gas at Room Temperature, *Diamond Relat. Mater.*, **124**: 108932 (2022).

[23] Singh R.S., Solanki A., Modulation of Electronic Properties of Silicon Carbide Nanotubes via Sulphur-Doping: An Ab Initio study, *Physics Letters A*, **380**: 1201-1204 (2016).

[24] Singh R.S., Hydrogen Adsorption on Sulphur-Doped SiC Nanotubes, *Mater. Res. Express*, **3(7)**: 075014 (2016).

[25] Singh R.S., Influence of oxygen Impurity on Electronic Properties of Carbon and Boron Nitride Nanotubes: A Comparative Study, *AIP Adv.*, **5(11)**: 117150 (2015).

[26] Umebayashi T., Yamaki T., Itoh H., Asai K., Analysis of Electronic Structures of 3d Transition Metal-Doped TiO_2 Based on Band Calculations, *J. Phys. Chem. Solids*, **63(10)**: 1909- 1920 (2002).

[27] Choi W., Termin A., Hoffmann M.R., The Role of Metal Ion Dopants in Quantum-Sized TiO_2: Correlation Between Photoreactivity and Charge Carrier Recombination Dynamics, *J. Phys. Chem*., **98(51)**: 13669- 13679 (1994).

[28] Cavalheiro A., Bruno J., Saeki M., Valente J., Florentino A., Effect of Scandium on the Structural and Photocatalytic Properties of Titanium Dioxide Thin Films, *J. Mater. Sci.*, **43(2)**: 602 (2008).

[29] Wei Z., Mei W., Xiyu S., Yachao W., Zhenyong L., Electronic and Optical Properties of the Doped TiO_2 System, *J. Semicond*., **31(7)**: 072001 (2010).

[30] Zabihi-Mobarakeh H,, Nezamzadeh-Ejhieh A., Application of Supported TiO_2 onto Iranian Clinoptilolite Nanoparticles in the Photodegradation of Mixture of Aniline and 2, 4-Dinitroaniline Aqueous Solution, *J. Ind. Eng. Chem*., **26**: 315-321 (2015).

[31] Piramoon S., Aberoomand Azar P., Saber Tehrani M., Optimization of Solar-Photocatalytic Degradation of Polychlorinated Biphenyls Using Photocatalyst ($Nd/Pd/TiO_2$) by Taguchi Technique and Detection by Solid Phase Nano Extraction, *Iran. J. Chem. Chem. Eng. (IJCCE)*, **40(5)**: 1541-1553 (2021).

[32] Janitabar Darzi S., Movahedi M., Visible Light Photodegradation of Phenol Using Nanoscale TiO_2 and ZnO Impregnated with Merbromin Dye: A Mechanistic Investigation, *Iran. J. Chem. Chem. Eng. (IJCCE)*, **33(2)**: 55-64 (2014).

[33] Sahraeian S., Alipour V., Heidari M., Rahmanian O., Karimi Abdolmaleki M., Application of Photocatalytic Process Using UV/TiO_2 for Degradation of Cefepime: A Comparison Between Photocatalytic and Photolytic, *Iran. J. Chem. Chem. Eng. (IJCCE)*, **40(3)**: 796-803 (2021).

[34] Perdew J.P., Burke K., Ernzerhof M., Generalized Gradient Approximation Made Simple, *Phys. Rev. Lett*., **77(18)**: 3865 (1996).

[35] Lee J.-Y., Park J., Cho J.-H., Electronic Properties of N-and C-Doped TiO_2, *Appl. Phys. Lett*., **87(1)**: 1904 (2005).

[36] Shao G., Electronic Structures of Manganese-Doped Rutile TiO_2 from First Principles, *J. Phys. Chem. C*, **112(47)**: 18677- 18685 (2008).